Preprints of the 21st IFAC World Congress (Virtual)
Berlin, Germany, July 12-17, 2020

Admittance matrix computation and stability analysis of droop controlled DC micro-grids with CPL ⋆

A.-C. Braitor, G.C. Konstantopoulos, V. Kadirkamanathan

Department of Automatic Control and Systems Engineering, The University of Sheffield, Sheffield, S1 3JD, UK (e-mail: abraitor1,g.konstantopoulos,visakan@sheffield.ac.uk).

Abstract: In this paper, an analytical method of computing the admittance matrix is introduced that facilitates the stability analysis of DC micro-grid systems, in presence of constant power loads (CPLs). Due to their nonlinear behaviour, CPLs can yield instability in DC micro-grids; an effect referred to as 'negative impedance instability'. The proposed method is particularly useful when a typical controller (droop control, voltage regulation) is designed to control the DC bus voltage of the micro-grid, as it allows the factorisation of the admittance matrix separating singular matrices. In doing so, the closed-loop stability proof can be more easily approached by isolating the singularities and, then employing straightforward linear algebra tools to arrive at the stability conditions. In order to validate the proposed approach, compute the admittance matrix and test the stability conditions, a DC micro-grid with n DC/DC power converters connected to a CPL is considered. Simulation results are also displayed to demonstrate the desired operation of the DC micro-grid control and design framework.

Keywords: DC micro-grids, admittance matrix, stability analysis, power converters.

1. INTRODUCTION

Seen as a capable technology to provide an efficient coupling between renewable energy sources (RES), energy storage systems and DC loads, DC micro-grids have recorded a significant increase in focus and interest. Compared to conventional AC frameworks, DC systems provide a higher efficiency and reliability, a simpler control structure and expandability, as well as a natural interface to the increased numbers of DC renewable generations, storage systems and electronic loads (Rashad et al., 2018).

In recent years, due to the widespread use of renewables as distributed generation units, the motivation for design and operation of DC micro-grids has significantly increased. Various applications (e.g. electronic devices, batteries or photovoltaic panels) can be directly connected to the DC network, mitigating energy conversion losses by reducing the multi AC/DC conversion stages and instability issues raised by the frequency and reactive power control. Their upsides have been confirmed in a wide range of industry applications, i.e. electric ships (Cairoli and Dougal, 2013), vehicles (Bosich et al., 2014), trains (Yoshida et al., 2017), and aircrafts (Magne et al., 2013). Apart from the development of industrial, commercial or residential DC distribution networks, several different promising DC framework applications can be found in EV charging stations or smart buildings (Zhang et al., 2015).

Control schemes in DC micro-grids are mainly designed to guarantee voltage regulation and accurate load power distribution, while maintaining system stability. However, the challenge of ensuring the stability of the system remains, as it is not always a straightforward problem. Therefore, most times stability is not rigorously addressed, mainly due to the complex dynamics that the system components and the nonlinear loads introduce. Constant power loads (CPLs), for instance, exhibit a negative impedance behaviour which makes the stabilisation problem much more complex.

The remaining of this section includes a brief literature review on CPLs previous studies, some state-of-the-art methods of computing admittance matrices and their present impact on the stability analysis in presence of nonlinear loads, followed by a list of the main contributions of this work and revisiting some common notations and preliminaries used throughout the paper. In Section 2, a standard configuration of a DC micro-grid is proposed for investigation, along with its corresponding admittance matrix in Section 3. Stability analysis is conducted in Section 4, for the closed-loop system with a droop controller, while simulations are displayed in Section 5. Finally, conclusions are drawn in Section 6.

1.1 Literature review

A widely employed strategy to guarantee voltage regulation and effective current (or power) sharing, without using communication, is to introduce a virtual resistance at the output of each converter, a method referred to as the droop control method, as in Karlsson and Svensson (2003); Mahmoodi et al. (2006); Huang et al. (2015). To address its shortcomings in terms of voltage regulation and power sharing accuracy trade-off, the droop control has been proposed in many forms, i.e. nonlinear droop

⋆ This work was supported by EPSRC under Grants No. EP/S001107/1 and EP/S031863/1.

(Cingoz et al., 2017), quadratic droop (Simpson-Porco et al., 2017), robust droop (Shuai et al., 2016). However, in order to ensure system stability with CPLs, in small-signal analysis, the impedance inequality criteria must be satisfied.

Passive damping methods are one type of approach to reshape the output impedance of the input filter by adding an extra physical resistance (Cespedes et al., 2011), but this creates additional power losses. Active damping methods, based on cascaded systems without input filters between two stage converters, were proposed to tackle this issue. Even though this approach is popular in small-scale micro-grids, for instance in electric vehicles (Magne et al., 2012), it is not applicable in relatively large DC micro-grids. Aside from these strategies, a significant deal of research articles has looked into the stability and stabilization methods of droop-controlled DC micro-grids with a single (Kwasinski and Onwuchekwa, 2011; Marx et al., 2012; Zhao et al., 2014), or multiple converter (Liu et al., 2011; Sulligoi et al., 2012; Anand and Fernandes, 2013; Tahim et al., 2015; Cupelli et al., 2015; Su et al., 2018) architecture feeding constant power loads. Due to the CPL negative impedance characteristic, the system tends to be unstable if traditional decentralized or distributed control is implemented independently.

In Anand and Fernandes (2013) and Tahim et al. (2015), the dynamics of the DC/DC power converters and the transient process are ignored, when the reduced order linearised model is derived. In Anand and Fernandes (2013), the stable ranges of the droop coefficients are obtained for the reduced-order model of a low-voltage DC micro-grid. Equivalently in Tahim et al. (2015), the safe operating regions are obtained for the simplified two-order RLC model system. Hence, these research works conclude that only if the droop coefficient is larger than the equivalent negative impedance CPL, the system would be stable. A wider stability region is obtained in (Su et al., 2018) considering a DC micro-grid described by the linear dynamics of the buck converters, but the method is only applicable to the conventional static droop control, which introduces the well-known limitations (inaccurate power sharing, significant load voltage drop).

Despite the many efforts to address this problem, proving closed-loop stability in the presence of CPLs continues to remain a non-trivial challenge, especially when a dynamic droop controller is applied at each unit of the micro-grid.

1.2 Main contributions

The main contributions of this paper are listed below:

(1) Admittance matrix: A new analytic method for computing and suitably factorising the admittance matrix of a DC micro-grid consisting of n sources and a CPL is presented, to provide the key tool for proving the system's stability.

(2) Closed-loop system model: Opposed to the typical static droop control concept, here a dynamic droop control architecture is considered for each one of the n units, which also includes the common DC bus voltage measurement that further complicates the analysis.

(3) Stability analysis: By employing the quadratic eigenvalue problem (QEP) theory to the closed-loop system and utilising the factorisation of the admittance matrix, analytic stability conditions are obtained to guide the control design.

(4) Validation: The proposed approach is then verified through simulation testing for a DC micro-grid with 5 DC/DC buck converters connected to common DC bus and feeding a CPL.

1.3 Notation and preliminaries

(1) Vectors and matrices

Let $\mathbf{1}_n \in \mathbf{R}^n$, $\mathbf{0}_n \in \mathbf{R}^n$ and $\mathbf{1}_{n\times n} \in \mathbf{R}^{n\times n}$, $\mathbf{0}_{n\times n} \in \mathbf{R}^{n\times n}$ be the n-dimensional vectors and square matrices with all elements equal to one and zero, respectively. Given an n-tuple sequence $(x_1, \ldots, x_n)$, let $x \in \mathbf{R}^n$ be the associated vector and $[x] \in \mathbf{R}^{n\times n}$ the diagonal matrix whose diagonal terms are the elements of the x. The identity matrix of size n is denoted by I_n.

(2) Linear matrix analysis

Lemma 1. Let $\lambda_1 \leq \lambda_2 \leq \cdots \leq \lambda_n$ represent the eigenvalues of a Hermitian matrix A, and $\beta_1 \leq \beta_2 \leq \cdots \leq \beta_n$ the eigenvalues of a Hermitian matrix B. Then, it holds that

$$\lambda_i + \beta_1 \leq \eta_i \leq \lambda_i + \beta_n$$

where $\eta_1 \leq \eta_2 \leq \cdots \leq \eta_n$ are the eigenvalues of the Hermitian matrix $A + B$.

Proof. Presented in Chapter 7, in Meyer (2000). □

Lemma 2. Let A be a positive-semidefinite Hermitian matrix, and D a positive-definite Hermitian matrix. Then

(a) Matrix product AD (or DA) is diagonalizable.
(b) If $A, D \in \mathbf{R}^{n\times n}$, the eigenvalues of AD (or DA) have only real part, and the product AD (or DA) has the same number of negative (zero, or positive) eigenvalues as matrix A.

Proof. By polar decomposition AD (or DA) is of the form $AD = UP$, where U is unitary and $P = \sqrt{(AD)^* AD}$ is a positive-semidefinite Hermitian matrix. Define Q unitary to meet $Q^2 = U$. Note that $M = Q^{-1}(AD)Q = QPQ$ is Hermitian, and by spectral decomposition $M = V\Lambda V^{-1}$, with V unitary and Λ diagonal with the eigenvalues of M (and same index of inertia as AD) on the main diagonal. It can be inferred that $(QV)^{-1} AD (QV) = \Lambda$, with QV unitary. Statement (a) is proved.

The similarity transformation $D^{\frac{1}{2}}(AD)D^{-\frac{1}{2}} = D^{\frac{1}{2}} A D^{\frac{1}{2}}$ is congruent to A; thus, according to Sylvester's law of inertia, AD has the same index of inertia as matrix A. The proof of conclusion (b) is presented in Chapter 7, in Meyer (2000). □

2. DC MICRO-GRID MODEL

The system under consideration is a typical DC micro-grid, depicted in Figure 1, consisting of n power converters connected in parallel to a common DC bus that feeds an equivalent constant power load.

By applying Kirchhoff's laws, the governing dynamic equations of the of the capacitor voltages, in matrix form, are the following

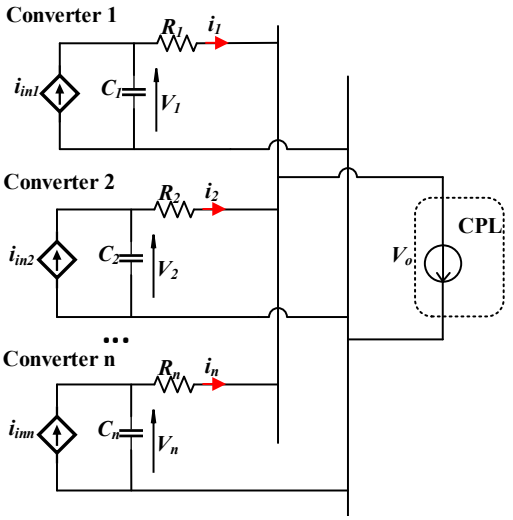

Fig. 1. Typical architecture of a DC micro-grid

$$C\dot{V} = i_{in} - i \tag{1}$$

where $C = diag\{C_i\}$, $V = [V_1 \dots V_n]^T$ represents the state vector capacitor voltages, $i = [i_1 \dots i_n]^T$ is the output current vector, and $i_{in} = [i_{in1} \dots i_{inn}]^T$ is the control input vector representing the current of each converter.

For constant power loads, the power balance equation should be satisfied, i.e.

$$V_o \sum_{i=1}^{n} i_i = P \tag{2}$$

where V_o represents the voltage of the DC bus, P is the power of the load, and i_i is defined as

$$i_i = \frac{V_i - V_o}{R_i} \tag{3}$$

with R_i being the resistance of the line/cable. Now, consider the following assumption:

Assumption 1. Let the following inequality hold

$$\left(\sum_{i=1}^{n} \frac{V_i}{R_i}\right)^2 > 4P \sum_{i=1}^{n} \frac{1}{R_i}. \tag{4}$$

with $P > 0$ *and* $V_i > 0$, $\forall i = 1, 2 \dots n$.

Thus, substituting the output current i_i from equation (3) into equation (2), one can obtain the following expression for the load voltage given by the real solutions of the second order polynomial

$$V_o = \frac{\sum_{i=1}^{n} \frac{V_i}{R_i} \pm \sqrt{\left(\sum_{i=1}^{n} \frac{V_i}{R_i}\right)^2 - 4P \sum_{i=1}^{n} \frac{1}{R_i}}}{2 \sum_{i=1}^{n} \frac{1}{R_i}} \tag{5}$$

The load voltage has two solutions, a high voltage and a low voltage, with the high voltage representing the feasible solution. This fact is also reported in Simpson-Porco et al. (2017) and Su et al. (2018). Therefore, the voltage of the load can be described as

$$V_o = \frac{\sum_{i=1}^{n} \frac{V_i}{R_i} + \sqrt{\left(\sum_{i=1}^{n} \frac{V_i}{R_i}\right)^2 - 4P \sum_{i=1}^{n} \frac{1}{R_i}}}{2 \sum_{i=1}^{n} \frac{1}{R_i}}. \tag{6}$$

Remark 1. System (1) represents a generic model of n-sourced units that could be integrated with the micro-grid via different power converter configurations (buck, boost, buck-boost, AC/DC) in the given DC micro-grid framework.

3. ADMITTANCE MATRIX

By taking the partial derivative of the output current i_i from (3) with respect to the capacitor voltage V_i, we obtain the admittance matrix

$$Y = \frac{\partial i_i}{\partial V_i} = \begin{bmatrix} \frac{1}{R_1}\left(1 - \frac{\partial V_o}{\partial V_1}\right) & -\frac{1}{R_1}\frac{\partial V_o}{\partial V_2} & \dots & -\frac{1}{R_1}\frac{\partial V_o}{\partial V_n} \\ -\frac{1}{R_2}\frac{\partial V_o}{\partial V_1} & \frac{1}{R_2}\left(1 - \frac{\partial V_o}{\partial V_2}\right) & \dots & -\frac{1}{R_2}\frac{\partial V_o}{\partial V_n} \\ \vdots & \vdots & \ddots & \vdots \\ -\frac{1}{R_n}\frac{\partial V_o}{\partial V_1} & -\frac{1}{R_n}\frac{\partial V_o}{\partial V_2} & \dots & \frac{1}{R_n}\left(1 - \frac{\partial V_o}{\partial V_n}\right) \end{bmatrix}$$

$$= \begin{bmatrix} \frac{1}{R_1} & 0 & \dots & 0 \\ 0 & \frac{1}{R_2} & \dots & 0 \\ \vdots & \vdots & \ddots & \vdots \\ 0 & 0 & \dots & \frac{1}{R_n} \end{bmatrix} \left(I_n - \begin{bmatrix} \frac{\partial V_o}{\partial V_1} & \frac{\partial V_o}{\partial V_1} & \dots & \frac{\partial V_o}{\partial V_1} \\ \frac{\partial V_o}{\partial V_2} & \frac{\partial V_o}{\partial V_2} & \dots & \frac{\partial V_o}{\partial V_2} \\ \vdots & \vdots & \ddots & \vdots \\ \frac{\partial V_o}{\partial V_n} & \frac{\partial V_o}{\partial V_n} & \dots & \frac{\partial V_o}{\partial V_n} \end{bmatrix} \right)$$

$$= \begin{bmatrix} \frac{1}{R_1} & 0 & \dots & 0 \\ 0 & \frac{1}{R_2} & \dots & 0 \\ \vdots & \vdots & \ddots & \vdots \\ 0 & 0 & \dots & \frac{1}{R_n} \end{bmatrix} \left(I_n - \mathbf{1}_{n \times n} \begin{bmatrix} \frac{\partial V_o}{\partial V_1} & 0 & \dots & 0 \\ 0 & \frac{\partial V_o}{\partial V_2} & \dots & 0 \\ \vdots & \vdots & \ddots & \vdots \\ 0 & 0 & \dots & \frac{\partial V_o}{\partial V_n} \end{bmatrix} \right)$$

$$= R^{-1}\left(I_n - \mathbf{1}_{n \times n} D\right) \tag{7}$$

where $R = diag\{R_i\}$ and $D = diag\{\frac{\partial V_o}{\partial V_i}\}$ with the following expression

$$D = \begin{bmatrix} \frac{\partial V_o}{\partial V_1} & \dots & 0 \\ \vdots & \ddots & \vdots \\ 0 & \dots & \frac{\partial V_o}{\partial V_n} \end{bmatrix} =$$

$$= \frac{1}{2\sum_{i=1}^{n} \frac{1}{R_i}} \left(R^{-1} + \frac{\sum_{i=1}^{n} \frac{V_i}{R_i}}{\sqrt{\left(\sum_{i=1}^{n} \frac{V_i}{R_i}\right)^2 - 4P \sum_{i=1}^{n} \frac{1}{R_i}}} \begin{bmatrix} \frac{1}{R_1} & \dots & 0 \\ \vdots & \ddots & \vdots \\ 0 & \dots & \frac{1}{R_n} \end{bmatrix} \right)$$

$$= \frac{1}{2\sum_{i=1}^{n} \frac{1}{R_i}} \left(R^{-1} + \frac{\sum_{i=1}^{n} \frac{V_i}{R_i}}{\sqrt{\left(\sum_{i=1}^{n} \frac{V_i}{R_i}\right)^2 - 4P \sum_{i=1}^{n} \frac{1}{R_i}}} R^{-1} \right)$$

where $\sqrt{\left(\sum_{i=1}^{n} \frac{V_i}{R_i}\right)^2 - 4P \sum_{i=1}^{n} \frac{1}{R_k}} > 0$ according to *Assumption 1.* Since R is a diagonal and positive-definite matrix, then it is clear that matrix D is a positive-definite diagonal matrix, with eigenvalues of the form

$$\lambda_{Di} = \frac{1}{2\sum_{i=1}^{n} \frac{1}{R_i}} \left(\frac{1}{R_i} + \frac{\sum_{i=1}^{n} \frac{V_i}{R_i}}{\sqrt{\left(\sum_{i=1}^{n} \frac{V_i}{R_i}\right)^2 - 4P \sum_{i=1}^{n} \frac{1}{R_i}}} \frac{1}{R_i} \right),$$

with $i = 1, \dots, n$.

Remark 2. In Su et al. (2018) and Liu et al. (2018), the power balance equation is linearized and then an expression for V_o is obtained with respect to its steady-state equilibrium, V_{oe}. This new expression of V_o is substituted in equation (3) and used to, finally, compute the admittance matrix as a function of the equilibrium point, V_{oe}, of the load voltage. On the contrary, here the proposed method considers the instantaneous nonlinear expressions of the output currents, i_i from (3), and the load voltage, V_o from (6), to compute the admittance matrix for every V_i. When the admittance matrix is required at a particular equilibrium point, then it can be calculated with $V_i = V_{ie}$, where V_{ie} is the value of the capacitor voltage at each node, i, at the equilibrium point.

4. STABILITY OF DROOP CONTROLLED MICRO-GRIDS

In the DC micro-grid under consideration, the main task is to achieve load voltage regulation close to a desired reference value and share the load proportionally to the sources capacities. This can be achieved through droop control operation as explained below.

4.1 Droop control design

Conventional droop controllers introduce a static structure and regulate the sources output voltage, which leads to significant load voltage drop and inaccurate power sharing. To improve the load voltage regulation and power sharing, a dynamic droop controller is introduced with the following expression

$$\dot{V} = V^*\mathbf{1}_n - V_o - mi, \tag{8}$$

with V^* being the reference voltage, and $m = diag\{m_i\}$ the droop coefficients. At the steady-state there is

$$V_o = V^* - m_i i_i, \tag{9}$$

which ensures accurate power sharing

$$m_1 i_1 = m_2 i_2 = \cdots = m_n i_n \tag{10}$$

proportionally to the sources capacities with suitable choice of m_i. The droop controller is implemented using a proportional integral (PI) controller, in matrix form, as follows,

$$i_{in} = -k_P V + \sigma \tag{11}$$

$$\dot{\sigma} = k_I \left(V^*\mathbf{1}_n - V_o - mi\right), \tag{12}$$

where $k_P = diag\{k_{Pi}\}$ and $k_I = diag\{k_{Ii}\}$ are the proportional and integral gains of the PI controller, respectively, and for which

$$m_i < R_i, \forall\, i \in \{1 \dots n\} \tag{13}$$

By replacing the controller dynamics (11)-(12) into the open-loop system (1), the closed-loop system becomes

$$C\dot{V} = -k_P V + \sigma - i \tag{14}$$

$$\dot{\sigma} = k_I \left(V^*\mathbf{1}_n - V_o - mi\right) \tag{15}$$

where i is linked to V through the impedance matrix.

4.2 Stability analysis

Consider an equilibrium point (V_e, σ_e) of the closed-loop system (14)-(15), (3) and (6), satisfying *Assumption 1.* Then the following Theorem can be formulated that guarantees stability of the entire droop-controlled DC micro-grid with a CPL.

Theorem 1. The equilibrium point (V_e, σ_e) is asymptotically stable if the following conditions holds

$$k_{Pi} > \frac{n\lambda_{Di} - 1}{R_i},\ \forall\, i \in \{1 \dots n\}. \tag{16}$$

Proof. The Jacobian matrix corresponding to system (14)-(15) takes the following form

$$J = \begin{bmatrix} -C^{-1}k_P - C^{-1}Y & C^{-1} \\ -k_I\mathbf{1}_{n\times n}D - k_I mY & \mathbf{0}_{n\times n} \end{bmatrix}.$$

Replacing the admittance matrix with its expression from (7), it yields

$$J = \begin{bmatrix} -C^{-1}k_P - C^{-1}R^{-1}\left(I_n - \mathbf{1}_{n\times n}D\right) & C^{-1} \\ -k_I\mathbf{1}_{n\times n}D - k_I mR^{-1}\left(I_n - \mathbf{1}_{n\times n}D\right) & \mathbf{0}_{n\times n} \end{bmatrix}.$$

The characteristic polynomial of the system can be written as

$$|\lambda I_{2n} - J| = |\lambda^2 I_n + \mathbf{C}\lambda + \mathbf{K}| = 0 \tag{17}$$

with

$$\mathbf{C} = C^{-1}k_P + C^{-1}R^{-1}\left(I_n - \mathbf{1}_{n\times n}D\right)$$

$$\mathbf{K} = C^{-1}\left(k_I mR^{-1} + k_I\left(I_n - mR^{-1}\right)\mathbf{1}_{n\times n}D\right)$$

By right multiplying (17) with $|D|^{-1} > 0$, the obtained determinant is

$$|\lambda^2 D^{-1} + \overline{\mathbf{C}}\lambda + \overline{\mathbf{K}}| = 0 \tag{18}$$

with

$$\overline{\mathbf{C}} = C^{-1}k_P D^{-1} + C^{-1}R^{-1}\left(D^{-1} - \mathbf{1}_{n\times n}\right)$$

$$\overline{\mathbf{K}} = C^{-1}\left(k_I mR^{-1}D^{-1} + k_I\left(I_n - mR^{-1}\right)\mathbf{1}_{n\times n}\right)$$

By left multiplying (18) with $|RC| > 0$, one obtains

$$|\lambda^2 RCD^{-1} + \tilde{\mathbf{C}}\lambda + \tilde{\mathbf{K}}| = 0 \tag{19}$$

with

$$\tilde{\mathbf{C}} = Rk_P D^{-1} + D^{-1} - \mathbf{1}_{n\times n}$$

being a symmetrical matrix and, following factorization,

$$\tilde{\mathbf{K}} = Rk_I\left(I_n - mR^{-1}\right)\left(\left(I_n - mR^{-1}\right)^{-1}R^{-1}mD^{-1} + \mathbf{1}_{n\times n}\right)$$

being a diagonalizable matrix whose eigenvalues are all real, according to *Lemma 2.* Hence, as $\tilde{\mathbf{K}}$ is represented by a product between a positive-definite diagonal and a symmetric matrix, there is $\tilde{\mathbf{K}} = P\Lambda P^{-1}$, where P is unitary and Λ is diagonal. The characteristic polynomial becomes

$$|\lambda^2 RCD^{-1} + \tilde{\mathbf{C}}\lambda + P\Lambda P^{-1}| = 0 \tag{20}$$

and, by left and right multiplication with $|P^{-1}|$ and $|P|$, respectively, it becomes

$$|\lambda^2 P^{-1}RCD^{-1}P + P^{-1}\tilde{\mathbf{C}}P\lambda + \Lambda| = 0 \tag{21}$$

Note that Λ is a diagonal matrix having the same index of inertia as $\tilde{\mathbf{K}}$ and the similarity transformations $P^{-1}RCD^{-1}P$ and $P^{-1}\tilde{\mathbf{C}}P$ are symmetrical, as P is unitary (orthogonal in $\mathbf{R}^{n\times n}$, $P^{-1} = P^T$), and they share the same eigenvalues as RCD^{-1}, and $\tilde{\mathbf{C}}$, respectively. If RCD^{-1}, $\tilde{\mathbf{C}}$ and Λ are positive-definite, then $Re\{\lambda\} < 0$, which means that matrix J is Hurwitz.

As RCD^{-1} is already positive-definite, it would suffice to show that $\tilde{\mathbf{C}} > 0$, and $\Lambda > 0$, or equivalently that $\tilde{\mathbf{K}}$ has positive eigenvalues.

(1) Condition $\tilde{\mathbf{C}} > 0$:

$$\tilde{\mathbf{C}} = Rk_P D^{-1} + D^{-1} - \mathbf{1}_{n\times n} > 0 \tag{22}$$

Since $\tilde{\mathbf{C}}$ is a sum of symmetric matrices, then according to *Lemma 1*, condition (22) can be rewritten in scalar form as

$$\frac{R_i k_{Pi}+1}{\lambda_{Di}} - n > 0, \forall\, i \in \{1 \dots n\}$$

which is always true, provided that (16) is satisfied.

(2) Condition $\Lambda > 0$, or $\tilde{\mathbf{K}}$ has positive eigenvalues: According to (13), the first matrix in the multiplication inside $\tilde{\mathbf{K}}$ is positive-definite, i.e.

$$Rk_I\left(I_n - mR^{-1}\right) > 0.$$

Hence, according to *Lemma 2*, one can investigate only the remaining (symmetrical) matrix in the product. This matrix

$$R^{-1}\left(I_n - mR^{-1}\right)^{-1} mD^{-1} + \mathbf{1}_{n\times n} > 0 \qquad (23)$$

is positive-definite since it is a sum between a positive-definite diagonal matrix and a positive semi-definite symmetrical matrix.

Hence, when (16) is satisfied, J is Hurwitz, and the equilibrium point (V_e, σ_e) is asymptotically stable. This completes the proof of *Theorem 1*. □

5. SIMULATION RESULTS

A DC micro-grid consisting of 5 parallel-operated buck converters, as depicted in Figure 2, with the parameters given in Table 1, and connected to a common DC bus with a CPL, has been simulated in Matlab/Simulink for $2\,s$.

Each converter is equipped with the droop controller considered in Section 4, and the task is to regulate the load voltage to the rated value, $V^* = 100\,V$, and share their output power in a $1:2:3:4:5$ ratio.

At $t = 0\,s$, the load power is $P = 500\,W$, and as one can see in Figure 3a, the load voltage is accurately fixed at $V_o = 99.9\,V$. The output currents satisfy their control

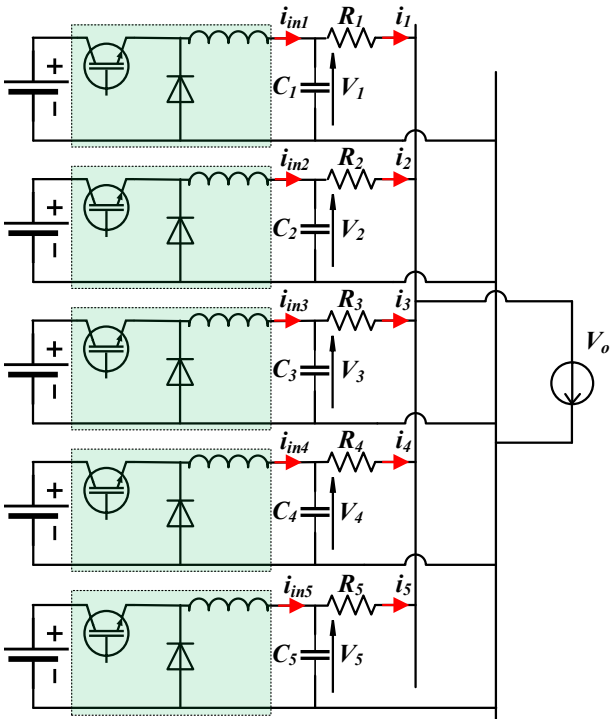

Fig. 2. DC micro-grid considered for testing

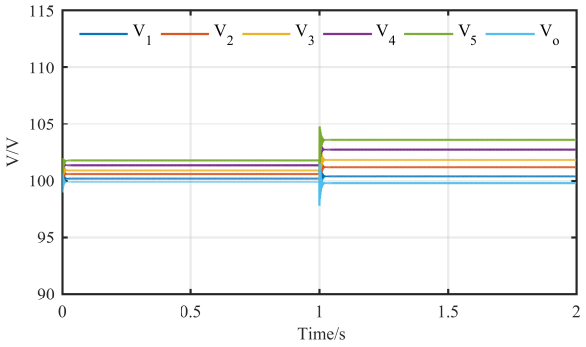

(a) Capacitor and load voltages

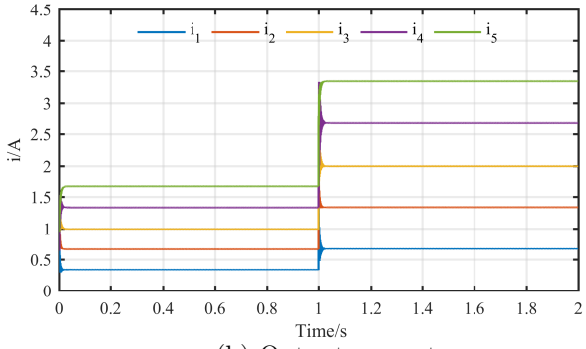

(b) Output currents

Fig. 3. Simulation results of the DC micro-grid system with PI controller

imposed ratios, having $i = [1.67\ \ 1.34\ \ 0.99\ \ 0.67\ \ 0.34]\,A$ (Figure 3b).

After one second, at $t = 1\,s$, the load power changes to $2P = 1\,kW$. The load voltage regulation is still fairly accurate, $V_o = 99.7\,V$ (Figure 3a), and, according to Figure 3b, the output currents respect their assigned proportions, having $i = [3.34\ \ 2.67\ \ 2.02\ \ 1.34\ \ 0.66]\,A$.

6. CONCLUSION

A novel approach to compute the admittance matrix has been proposed that facilitates the stability analysis, especially in the case where the controller aims to regulate the converter output voltage. Following the proposed strategy, after several factorisations, the isolation of singularities is possible, and henceforth, by employing straightforward linear algebra tools, the stability conditions can be comfortably acquired. A DC micro-grid consisting of 5 parallel-operated DC/DC buck converters feeding a common CPL has been used for testing and validating the proposed analysis. The results confirm that the presented strategy ensures normal operation of the DC network and guarantees an elementary path in ensuring closed-loop stability.

Table 1. System and control parameters

System Parameters	Values	System Parameters	Values
C_1	$110\mu F$	R_1	1Ω
C_2	$150\mu F$	R_2	1.1Ω
C_3	$100\mu F$	R_3	1.05Ω
C_4	$420\mu F$	R_4	1.12Ω
C_5	$200\mu F$	R_5	1.15Ω
Control Parameters	**Values**	**Control Parameters**	**Values**
m_1	0.42	m_5	0.084
m_2	0.21	$k_{P1\dots5}$	0.01
m_3	0.14	$k_{I1\dots5}$	2×10^3
m_4	0.105	V^*	100

REFERENCES

Anand, S. and Fernandes, B.G. (2013). Reduced-order model and stability analysis of low-voltage DC microgrid. *IEEE Transactions on Industrial Electronics*, 60(11), 5040–5049. doi:10.1109/TIE.2012.2227902.

Bosich, D., Giadrossi, G., Sulligoi, G., Grillo, S., and Tironi, E. (2014). More electric vehicles DC power systems: A large signal stability analysis in presence of CPLs fed by floating supply voltage. In *2014 IEEE International Electric Vehicle Conference (IEVC)*, 1–6. doi:10.1109/IEVC.2014.7056226.

Cairoli, P. and Dougal, R.A. (2013). New horizons in DC shipboard power systems: New fault protection strategies are essential to the adoption of DC power systems. *IEEE Electrification Magazine*, 1(2), 38–45. doi:10.1109/MELE.2013.2291431.

Cespedes, M., Xing, L., and Sun, J. (2011). Constant-power load system stabilization by passive damping. *IEEE Transactions on Power Electronics*, 26(7), 1832–1836. doi:10.1109/TPEL.2011.2151880.

Cingoz, F., Elrayyah, A., and Sozer, Y. (2017). Plug-and-play nonlinear droop construction scheme to optimize islanded microgrid operations. *IEEE Transactions on Power Electronics*, 32(4), 2743–2756. doi: 10.1109/TPEL.2016.2574202.

Cupelli, M., Mirz, M., and Monti, A. (2015). Application of backstepping to mvdc ship power systems with constant power loads. In *2015 International Conference on Electrical Systems for Aircraft, Railway, Ship Propulsion and Road Vehicles (ESARS)*, 1–6. doi: 10.1109/ESARS.2015.7101469.

Huang, P.H., Liu, P.C., Xiao, W., and Moursi, M.S.E. (2015). A novel droop-based average voltage sharing control strategy for DC microgrids. *IEEE Transactions on Smart Grid*, 6(3), 1096–1106. doi: 10.1109/TSG.2014.2357179.

Karlsson, P. and Svensson, J. (2003). DC bus voltage control for a distributed power system. *IEEE Transactions on Power Electronics*, 18(6), 1405–1412. doi: 10.1109/TPEL.2003.818872.

Kwasinski, A. and Onwuchekwa, C.N. (2011). Dynamic behavior and stabilization of dc microgrids with instantaneous constant-power loads. *IEEE Transactions on Power Electronics*, 26(3), 822–834. doi: 10.1109/TPEL.2010.2091285.

Liu, X., Zhou, Y., Zhang, W., and Ma, S. (2011). Stability criteria for constant power loads with multistage *lc* filters. *IEEE Transactions on Vehicular Technology*, 60(5), 2042–2049. doi:10.1109/TVT.2011.2148133.

Liu, Z., Su, M., Sun, Y., Han, H., Hou, X., and Guerrero, J.M. (2018). Stability analysis of DC microgrids with constant power load under distributed control methods. *Automatica*, 90, 62 – 72. doi: 10.1016/j.automatica.2017.12.051.

Magne, P., Nahid-Mobarakeh, B., and Pierfederici, S. (2012). General active global stabilization of multiloads dc-power networks. *IEEE Transactions on Power Electronics*, 27(4), 1788–1798. doi: 10.1109/TPEL.2011.2168426.

Magne, P., Nahid-Mobarakeh, B., and Pierfederici, S. (2013). Active stabilization of DC microgrids without remote sensors for more electric aircraft. *IEEE Transactions on Industry Applications*, 49(5), 2352–2360. doi: 10.1109/TIA.2013.2262031.

Mahmoodi, M., Gharehpetian, G.B., Abedi, M., and Noroozian, R. (2006). Control systems for independent operation of parallel DG units in DC distribution systems. In *2006 IEEE International Power and Energy Conference*, 220–224. doi: 10.1109/PECON.2006.346650.

Marx, D., Magne, P., Nahid-Mobarakeh, B., Pierfederici, S., and Davat, B. (2012). Large signal stability analysis tools in dc power systems with constant power loads and variable power loads—a review. *IEEE Transactions on Power Electronics*, 27(4), 1773–1787. doi: 10.1109/TPEL.2011.2170202.

Meyer, C.D. (2000). *Matrix Analysis and Applied Linear Algebra*. Society for Industrial and Applied Mathematics, Philadelphia.

Rashad, M., Raoof, U., Ashraf, M., and Ahmed, B. (2018). Proportional load sharing and stability of DC microgrid with distributed architecture using SM controller. *Mathematical Problems in Engineering*, 2018, 1–16. doi: 10.1155/2018/2717129.

Shuai, Z., He, D., Fang, J., Shen, Z.J., Tu, C., and Wang, J. (2016). Robust droop control of DC distribution networks. *IET Renewable Power Generation*, 10(6), 807–814. doi:10.1049/iet-rpg.2015.0455.

Simpson-Porco, J.W., Dörfler, F., and Bullo, F. (2017). Voltage stabilization in microgrids via quadratic droop control. *IEEE Transactions on Automatic Control*, 62(3), 1239–1253. doi:10.1109/TAC.2016.2585094.

Su, M., Liu, Z., Sun, Y., Han, H., and Hou, X. (2018). Stability analysis and stabilization methods of DC microgrid with multiple parallel-connected DC-DC converters loaded by CPLs. *IEEE Transactions on Smart Grid*, 9(1), 132–142. doi:10.1109/TSG.2016.2546551.

Sulligoi, G., Bosich, D., Zhu, L., Cupelli, M., and Monti, A. (2012). Linearizing control of shipboard multi-machine mvdc power systems feeding constant power loads. In *2012 IEEE Energy Conversion Congress and Exposition (ECCE)*, 691–697. doi:10.1109/ECCE.2012.6342753.

Tahim, A.P.N., Pagano, D.J., Lenz, E., and Stramosk, V. (2015). Modeling and stability analysis of islanded DC microgrids under droop control. *IEEE Transactions on Power Electronics*, 30(8), 4597–4607. doi: 10.1109/TPEL.2014.2360171.

Yoshida, Y., Figueroa, H.P., and Dougal, R.A. (2017). Comparison of energy storage configurations in railway microgrids. In *2017 IEEE Second International Conference on DC Microgrids (ICDCM)*, 133–138. doi: 10.1109/ICDCM.2017.8001034.

Zhang, F., Meng, C., Yang, Y., Sun, C., Ji, C., Chen, Y., Wei, W., Qiu, H., and Yang, G. (2015). Advantages and challenges of DC microgrid for commercial building a case study from Xiamen university DC microgrid. In *2015 IEEE First International Conference on DC Microgrids (ICDCM)*, 355–358. doi: 10.1109/ICDCM.2015.7152068.

Zhao, Y., Qiao, W., and Ha, D. (2014). A sliding-mode duty-ratio controller for DC/DC buck converters with constant power loads. *IEEE Transactions on Industry Applications*, 50(2), 1448–1458. doi: 10.1109/TIA.2013.2273751.